# Planar Multi Notch Band Antenna In-Band Gain Enhanced by Epsilon-Near-Zero Non-Absorptive Metasurface

**Priyanka Usha[1], Niraj Kumar[2, *], and Chitra Krishnan[2]**

**Abstract**—This paper presents the design, fabrication, and characterization of a novel single layer non-absorbing metasurface with a broadband epsilon near zero (ENZ) property and its application in-band gain enhancement of triple notch band ultra-wideband (UWB) antenna. The proposed metasurface is made up of non-resonant metamaterial unit cells consisting of half ring slots in a circular patch on an FR4 dielectric substrate. Metasurface with unit cells arranged in a $2 \times 2$ lattice pattern is suspended $4\,\text{mm}$ above the triple notch band antenna. The transmission and reflection properties of the metamaterial unit cell are analysed and optimised to ensure the coherent transmission from the metasurface. The non-absorbing property of the metasurface results in the minimal loss of electromagnetic waves. The proposed antenna system with metasurface has a size of $28 \times 28 \times 7.2\,\text{mm}^3$. The measured results of fabricated antenna are compared with the simulated ones and are in good match. The results show that the gain of the antenna was enhanced by $1.3\,\text{dB}$, $2.8\,\text{dB}$, and $4\,\text{dB}$ at $5\,\text{GHz}$, $7\,\text{GHz}$, and $9\,\text{GHz}$, respectively.

## 1. INTRODUCTION

The allocation of the UWB spectrum (3.1 to 10.6 GHz) for commercial communication purposes by the US Federal Communications Commission (FCC) in the year 2002 resulted in the increased demand of notch band antennas to overcome the problem of in-band electromagnetic interference (EMI). The most preferable designs presented for this purpose are printed antennas due to their low profile, planar structure, light weight, and ease of fabrication [1, 2]. It is noticed that obtaining high gain in printed notch band antennas is quite difficult. Array of antennas [3] is a technique commonly used for gain enhancement, but it results in large antenna size, high cost, and complexity of feed network. Recent methods like Fabry-Perot cavity antenna [4–7] and frequency selective surface (FSS) [8–11] can overcome this complexity, but they do not provide broadband gain enhancement. The latest solution for obtaining the broadband gain is to utilise artificial materials called metamaterials [12–15]. A periodic planar arrangement of metamaterial unit cells called metasurface can control electromagnetic properties like reflection, transmission, and absorption. Artificial intelligence and advanced materials are also being explored for the gain enhancement of antennas [16, 17]. It is found that the planar metasurfaces with metamaterial unit cells having near zero permeability and near zero permittivity help in increasing the efficiency, bandwidth, and gain of antennas [18–20]. 3-D Metamaterial lenses have also been used for the high gain and broadband performances by concentrating the radiated energy in the desired direction. The bulky and multilayer complicated structure of 3-D metamaterial might be expensive; hence planar structures are preferred [21, 22]. Single layer ENZ metasurfaces [23] are the new substitute to the bulky lenses. The phase shifting concept proposed in [24, 25] also provides broadband gain enhancement. All these broadband gain enhancement techniques can be utilized for multiband gain enhancement too [26, 27].

* Corresponding author: Niraj Kumar (nirajkumar@vit.ac.in).

[1] Department of Engineering Design, Indian Institute of Technology Madras, Chennai, India. [2] School of Electronics Engineering, Vellore Institute of Technology Chennai, India.

In this paper, a planar single layer metasurface is designed and applied to enhance the in-band gain of a triple notch band UWB antenna. To achieve this in-band gain enhancement, a new metamaterial unit cell with ENZ and non-absorptive property over a broad range of frequency is designed. Metamaterial unit cells are arranged to design the metasurface and suspended above a triple notch band antenna to get a coherent transmission and very low absorption loss. Metamaterial unit cell design and analysis is explained in Section 2, followed by metasurface design and elaborated radiation mechanism to enhance the antenna gain in Section 3. The simulated and experimental results of proposed design are presented and discussed in Section 4. The proposed work is concluded in Section 5.

## 2. METAMATERIAL UNIT CELL DESIGN AND ANALYSIS

Unit cell of the proposed metamaterial consists of a circular patch of radius 4.5 mm and two half ring slots of outer radius 4 mm and inner radius 3 mm designed on an FR4 substrate of dimension 14 mm × 14 mm as shown in Fig. 1(a). The optimized values of design parameters are tabulated in Table 1. Metamaterial unit cell analysis is done using ANSYS HFSS.

To get the reflection properties of metamaterial, periodic boundary condition (PBC) has been
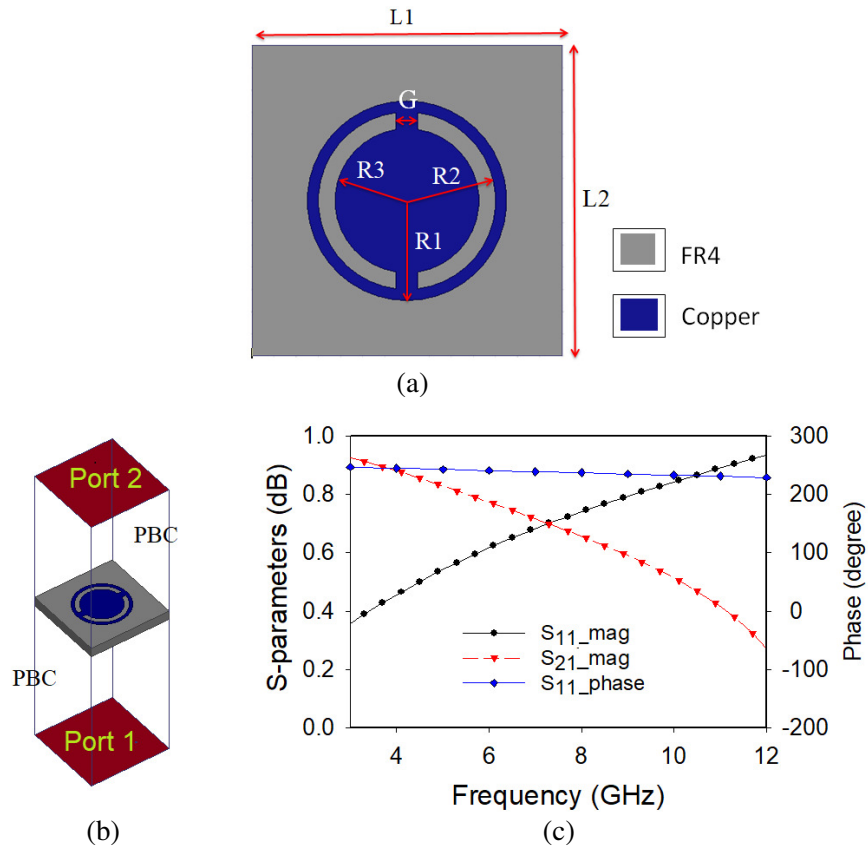


**Figure 1.** (a) Metamaterial unit cell design. (b) Unit cell analysis setup. (c) Magnitude and phase of reflection and transmission coefficient.

**Table 1.** Optimized values of parameters of unit cell.

| Parameters | $R_1$ | $R_2$ | $R_3$ | $L_1$ | $L_2$ | $G$ |
|---|---|---|---|---|---|---|
| values (mm) | 4.5 | 4 | 3 | 14 | 14 | 1 |

applied to unit cell. Perfect electric conductor (PEC) and perfect magnetic conductor (PMC) boundary conditions are applied along the $X$- and $Y$-axes, respectively, with the normal ($Z$-axis) incident field. Simulation setup for unit cell is shown in Fig. 1(b). After simulation we get reflection and transmission parameters as shown in Fig. 1(c). It is clear from the plots that unit cell does not resonate in UWB frequency region, and it has small and steady variation in phase of reflection over a wide range of frequency. Cutting two half ring slots in the circular patch changes the overall impedance and resonance properties of the structure by adding additional capacitance and inductance. Various models have been presented in literature to predict the behaviour of the metamaterial unit cells [22, 28–30]. The field distribution within the patch structure also gets modified, and it leads to changes in the effective permittivity permeability of the unit cell. With the simulated scattering parameters from metamaterial unit cell, the effective dielectric parameters are calculated [31] and plotted in MATLAB as shown in Fig. 2. Permittivity ($\epsilon$) and permeability ($\mu$) can be calculated as Eq. (1).

$$\epsilon = \frac{n}{z} \quad \text{and} \quad \mu = nz \tag{1}$$

where $n$ is refractive index, and $z$ is the wave impedance. These parameters are calculated using $S$-parameter presented in Fig. 1(c), as Eq. (2) and Eq. (3).

$$z = \pm\sqrt{\frac{(1+r^2)-t^2}{(1-r^2)-t^2}} \tag{2}$$

$$n = \left(\frac{\cos^{-1}\left(\frac{1}{2t}\left[1-(r^2-t^2)\right]\right)}{kd}\right) \tag{3}$$
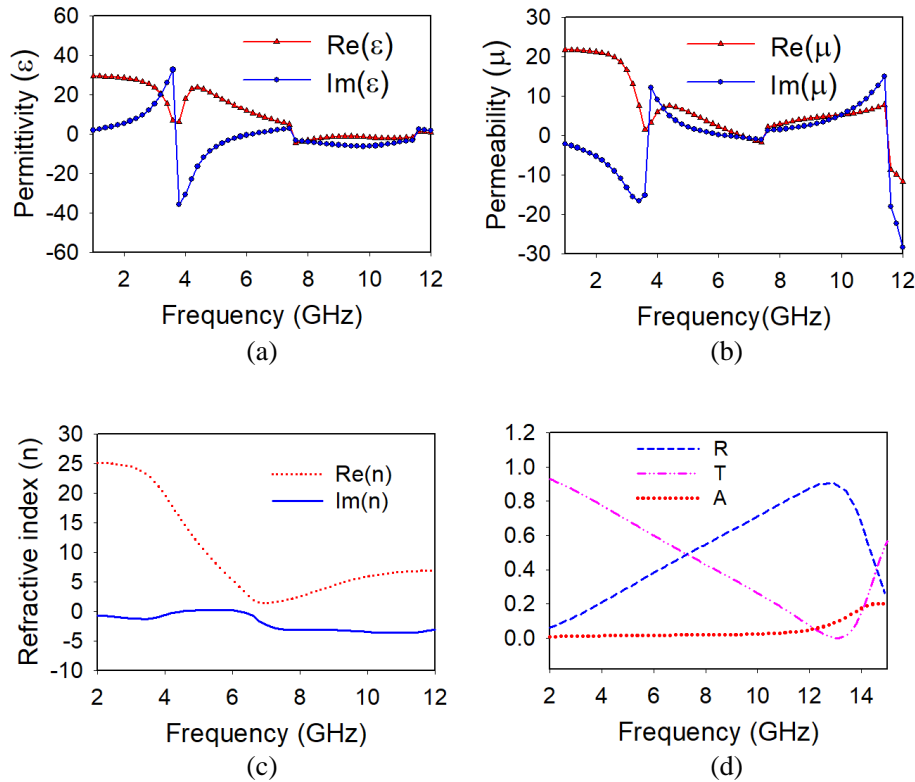


**Figure 2.** Real and imaginary part of effective, (a) permittivity and (b) permeability, (c) refractive index, (d) the reflectivity ($R$) and transmissivity ($T$) and absorptivity ($A$) curves.

where $r$ is the reflection coefficient, $t$ the transmission coefficient, $k$ the wave number, and $d$ the thickness of the metasurface slab.

The permittivity curve plotted in Fig. 2(a) validates that there is no resonance in UWB frequency region as the real part of permittivity monotonically decreases and becomes almost zero. Permeability curve plotted in Fig. 2(b) shows very low values for real and imaginary parts which indicate a weak dispersive magnetic loss. Hence, we get control over effective parameters for whole UWB frequency range by working in non-resonant region. Real and imaginary parts of refractive index are shown in Fig. 2(c). The imaginary part of refractive index is responsible for the attenuation of electromagnetic wave (EM) passing through the medium. Positive value of imaginary part of refractive index indicates loss. We get either near zero or negative value for the whole range. It means that the EM wave passes through the metamaterial without loss where the imaginary part of refractive index is near zero and gets amplified for a negative value. The reflectivity ($R$) and transmissivity ($T$) are given by Eq. (4) and Eq. (5), respectively [32]. Absorptivity ($A$) is calculated by Eq. (6), and curves are plotted in Fig. 2(d). We get an ultra-wideband non-absorptive property for the proposed metamaterial unit cell. Hence, the proposed metamaterial with ENZ property ensures very low loss and also contributes to EM wave amplification.

$$R = |r|^2 \tag{4}$$
$$T = |t|^2 \tag{5}$$
$$A = 1 - (R + T) \tag{6}$$

## 3. METASURFACE DESIGN AND IMPLEMENTATION IN ANTENNA GAIN ENHANCEMENT

The reference antenna used in this work is a planar UWB antenna with triple band notch characteristics for EMI reduction for WiMAX (3.5 GHz), WLAN (5.5 GHz), and X-band satellite down-link frequency (7.5 GHz) which occupy frequency bands within the designated UWB bandwidth [1]. The antenna is designed with a half-circular radiating patch having a radius of 14 mm on an FR4 substrate of 28 mm × 28 mm dimension to match the size of the metasurface. Antenna design with optimized parameters is shown in Fig. 3. The optimized value of the parameters of the antenna is tabulated in Table 2. A metasurface of 28 mm × 28 mm is designed and fabricated on an FR4 (dielectric constant
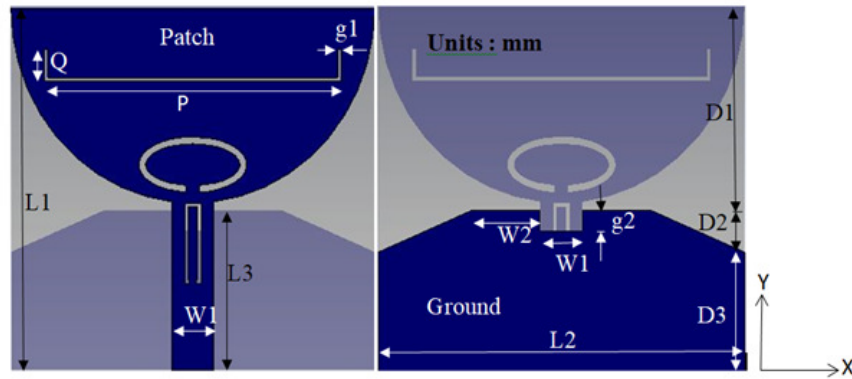


**Figure 3.** Reference antenna: Front and back view of antenna design.

**Table 2.** Optimized values of parameters of triple notch band UWB antenna.

| Parameters | $L_1$ | $L_2$ | $L_3$ | $P$ | $Q$ | $g_1$ | $g_2$ | $D_1$ | $D_2$ | $D_3$ | $W_1$ | $W_2$ |
|---|---|---|---|---|---|---|---|---|---|---|---|---|
| values (mm) | 28 | 28 | 11.5 | 22 | 1.75 | 0.25 | 1.5 | 16.5 | 4 | 7.5 | 3 | 5 |
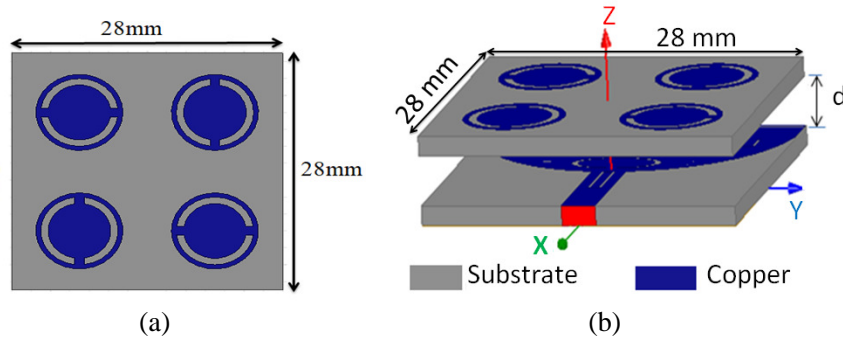
**Figure 4.** (a) Metasurface design consisting $2 \times 2$ unit cells and (b) simulated structure with feed, metasurface and antenna ($d = 4\,\text{mm}$).

4.4) substrate with the thickness of 1.6 mm. It consists of a $2 \times 2$ array of the proposed metamaterial unit cell as shown in Fig. 4(a). The metasurface is placed at a distance of 4 mm above the antenna for gain enhancement as shown in Fig. 4(b). $2 \times 2$ arrangement of the unit cells is best suited for keeping the size of the metasurface the same as the size of the antenna. The presented unit cell possesses a unique transmission property that can be used if it is placed above the antenna in the direction of maximum radiation of antenna.

Antenna radiation mechanism with metasurface is shown in Fig. 5(a). Electromagnetic wave radiated from source antenna hits the metasurface. Transmission and reflection phenomena occur as some portion of the radiated wave passes through the metasurface, and some gets reflected back and remains getting absorbed. Since the absorptivity of the proposed metamaterial is very low for the desired UWB frequency region, the entire radiation phenomenon is controlled mainly by reflected and transmitted EM waves. Also, the non-absorptive property helps to keep the absorption loss very low. The reflected wave from metasurface hits the antenna patch or ground and bounces back to the metasurface. To get enhanced gain of antenna, all the waves passing through the metasurface should be coherent. Phase difference ($\phi$) between the direct transmission and transmission after one reflection is calculated by Eq. (7), and the air gap between the antenna and metasurface is optimized for coherent transmission.

$$\phi = \theta + 180° + 2 \cdot \beta d \tag{7}$$

In the above setup, the total phase change is the summation of angle of reflection from unit cell ($\theta$), phase change due to air gap between the antenna and metasurface ($\beta d$), and reflection from ground plane ($180°$). Unit cell of the metamaterial is analysed by applying the boundary conditions for periodicity. There is coherent emergence of EM wave from the metasurface at $d = 4\,\text{mm}$ as the total phase difference
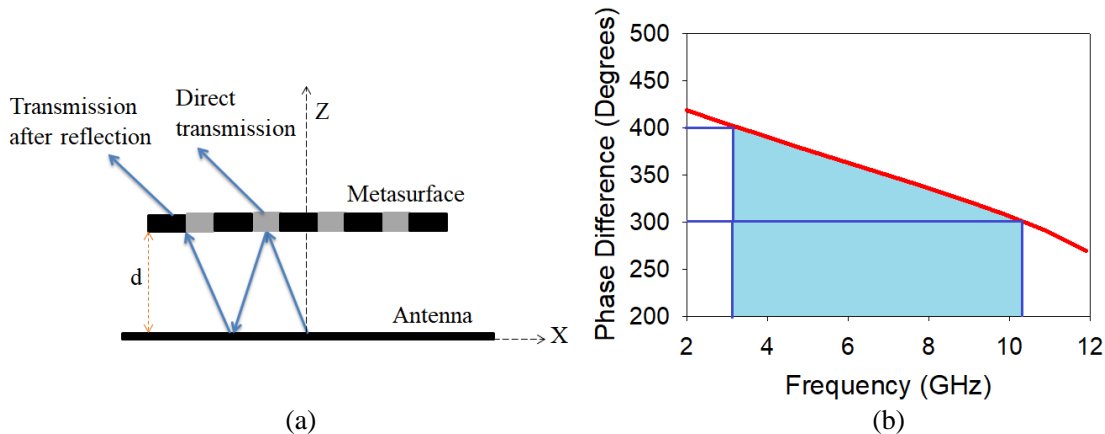


**Figure 5.** (a) Antenna radiation mechanism with metasurface ($d = 4\,\text{mm}$). (b) Phase difference analysis of EM wave emerging from metasurface.

is varied from $300°$ to $400°$ (very near $360°$) for the whole range of UWB ($3.1$–$10.6\,\mathrm{GHz}$) as plotted in Fig. 5(b).

## 4. RESULTS AND DISCUSSION

The entire antenna structure consisting of the feed, metasurface, and antenna, as shown in Fig. 3 with radiation boundary is simulated with ANSYS HFSS software. Finite element method (FEM) in HFSS solver is used for simulating the antenna structure with and without metasurface. The distance between antenna and metasurface is optimized and fixed as $d = 4\,\mathrm{mm}$. Antenna prototype is fabricated with photolithographic process. Choosing FR4 material as the substrate of antenna reduces the cost of the fabrication. Front and back views of the fabricated prototype of antenna are presented in Fig. 6(a) and Fig. 6(b). The printed prototype of metasurface was aligned and secured above the printed antenna with the help of double sided tape. Fig. 6(c) shows the setup for measurement inside the anechoic chamber. A horn antenna with UWB radiation property is used as the reference antenna and is kept at far field distance in the line of sight of test antenna. Simulated and measured return losses for antenna without and with metasurface are compared in Fig. 7(a) and Fig. 7(b), respectively. The triple notch band property of antenna for WiMAX ($3.5\,\mathrm{GHz}$), WLAN ($5.5\,\mathrm{GHz}$), and X-band satellite down-link frequency ($7.5\,\mathrm{GHz}$) does not get disturbed except small frequency shifts due to metasurface. Measured return loss is in good match with simulated result.
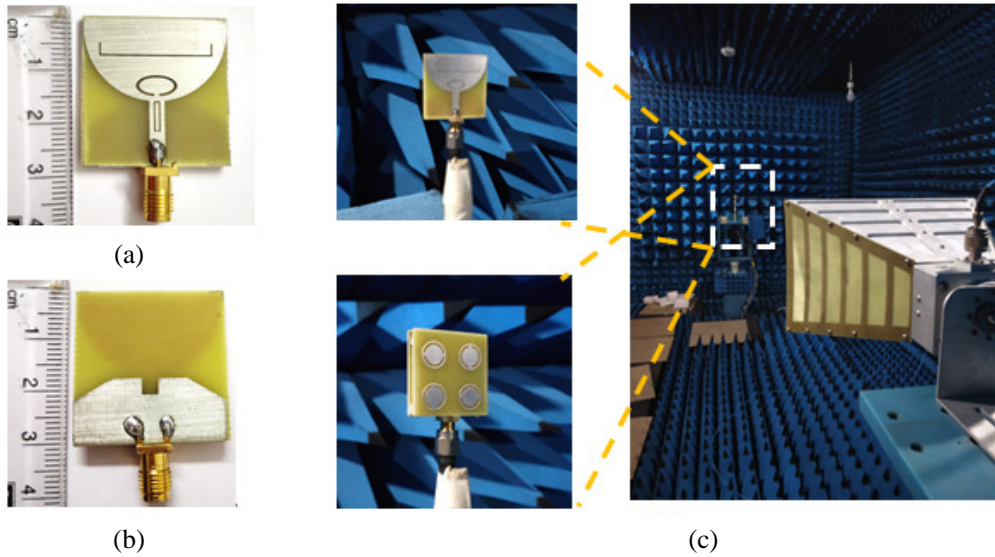


**Figure 6.** (a) Front view and (b) back view of fabricated prototype of antenna, (c) anechoic chamber setup for measurement.

Simulated gains for antenna with and without metasurface are plotted in Fig. 7(c). Gain enhancement of $1.3\,\mathrm{dB}$, $2.8\,\mathrm{dB}$, and $4\,\mathrm{dB}$ is achieved at $5\,\mathrm{GHz}$, $7\,\mathrm{GHz}$, and $9\,\mathrm{GHz}$, respectively. Maximum gain enhancement is $4\,\mathrm{dB}$ at $9\,\mathrm{GHz}$. Measured gains for antenna with and without metasurface are plotted in Fig. 7(d). Measured results give gain enhancement of $1.8\,\mathrm{dB}$ for $5\,\mathrm{GHz}$, $3\,\mathrm{dB}$ for $7\,\mathrm{GHz}$, and $3.9\,\mathrm{dB}$ for $9\,\mathrm{GHz}$. The minor discrepancies between the simulated and measured results can be minimized by reducing fabrication imperfections and rectifying antenna placement, calibration, and measurement equipment limitations. $E$-plane and $H$-plane radiation patterns of the antenna with and without metasurface at $6.5\,\mathrm{GHz}$ are plotted in Fig. 8(a) and Fig. 8(b). It can be noticed that the application of metasurface results in reduced back radiation and increased front radiation which improves the gain of the antenna. Hence, shaping of antenna radiation pattern is done using the proposed metasurface. Radiation efficiencies of antenna with and without metasurface are compared in Fig. 9. Radiation efficiency of more than $80\%$ is achieved for radiating bands. The comparison of
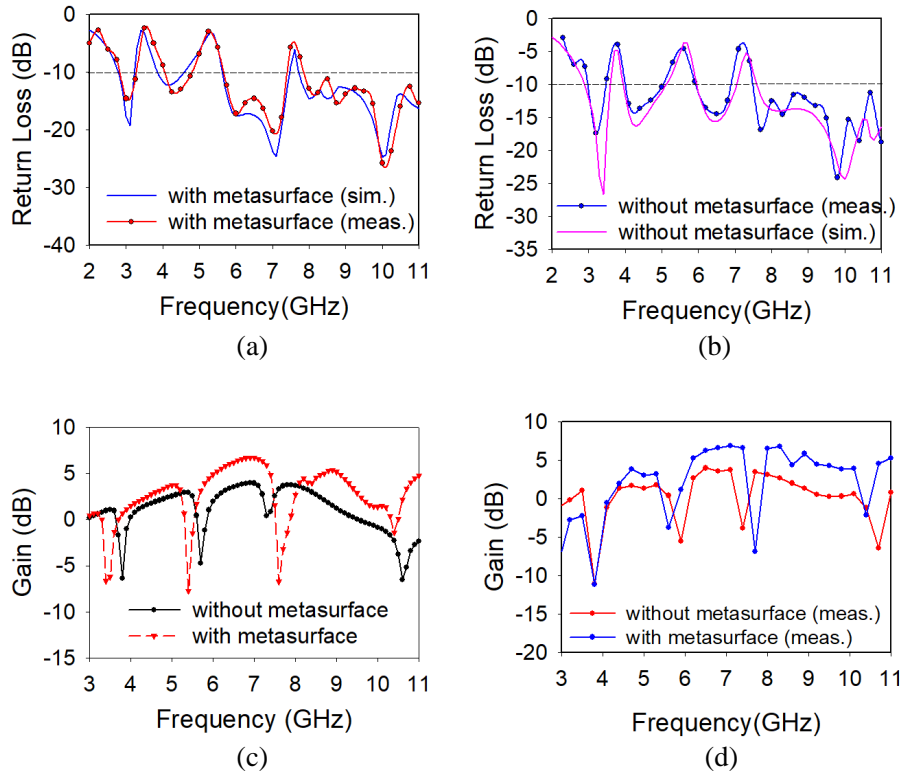
**Figure 7.** Comparison of (a) simulated and measured return loss with metasurface, (b) simulated and measured return loss without metasurface, (c) simulated gain, (d) measured gain.
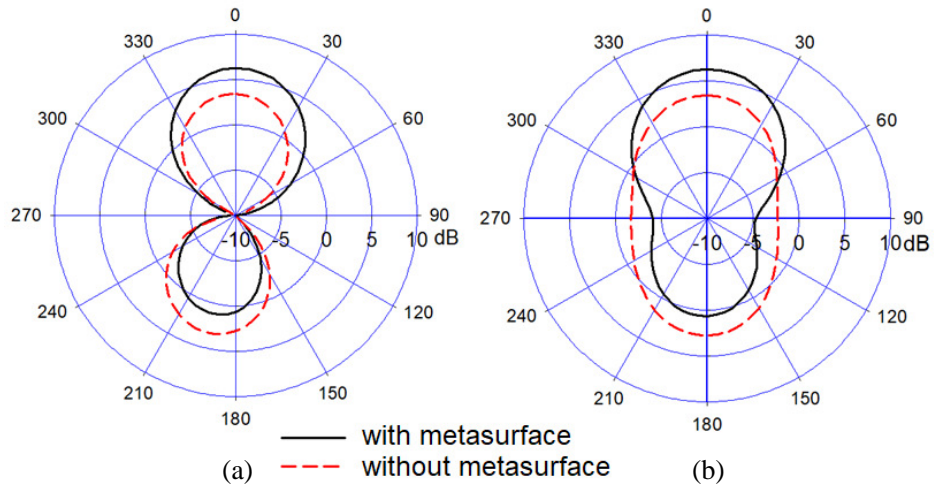


**Figure 8.** 2-D radiation pattern of antenna with and without metasurface for (a) $E$-plane and (b) $H$-plane at 6.5 GHz.

proposed work with recent works for gain enhancement in Table 3 shows that the proposed antenna system is compact in size and gives triple band notch property with significant enhancement in gain. As the gain of the antenna is still low at lower frequency range, this work gives the future scope of further improving the gain of the antenna in the lower frequency bands. The proposed antenna system has good futuristic application possibilities in internet of things and energy harvesting.
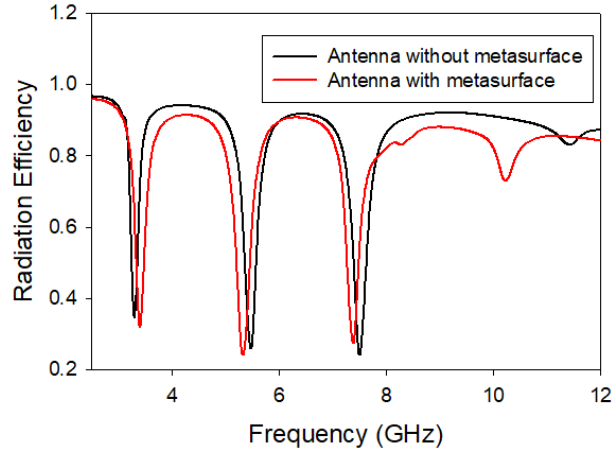
**Figure 9.** Radiation efficiency of antenna with and without metasurface.

**Table 3.** Comparison of proposed work with existing works.

| Ref. no. | Material used ($\epsilon_r$) | Antenna size (mm$^3$) | Freq. (GHz) | Max. gain enhancement (dB) |
|---|---|---|---|---|
| Ref. [7] | 4.4 | $20 \times 20 \times 0.8$ | 3.7–11 | 3 |
| Ref. [18] | 2.2 | $50 \times 75 \times 10$ | 5.5–7.8 | 5–6.5 |
| Ref. [24] | 4.4 | $\pi(89)^2 \times 68.7$ | 5.8 | 4.76 |
| Ref. [26] | 4.4 | $55 \times 55 \times 1.6$ | 2.5 | 3.69 |
| Ref. [27] | 4.4 | $64 \times 64 \times 4.9$ | 3.3, 5.9, 9 | 2.39, 3, 3.58 |
| This work | 4.4 | $28 \times 28 \times 7.2$ | 5, 7, 9 | 1.3, 2.8, 4 |

## 5. CONCLUSION

A novel metamaterial with unique ENZ material properties for a broadband frequency range is designed, and its application for antenna gain enhancement is successfully demonstrated in this paper. The unit cell of metamaterial consists of a circular patch with two half ring slots, and it is designed on a low cost FR4 substrate. Periodic boundary conditions are applied to unit cell analysis in HFSS. Reflection and transmission properties are analysed, and dielectric material properties are also extracted. The proposed metamaterial shows Epsilon near zero property and non-absorptive nature for UWB range of frequency. A compact single layer metasurface is designed with arranging four unit cells in a plane, and it is placed above a reference triple band notch UWB antenna at a appropriate gap to produce coherent radiation from the setup. Electromagnetic waves passing through the metasurface gets amplified due to the epsilon near zero and negative refractive index of the metamaterial. The non-absorptive nature of metamaterial ensures low loss of electromagnetic wave inside the material. Significant antenna gain enhancement is achieved for the radiation bands of the triple notch band UWB antenna. Radiation characteristics of antenna with and without metasurface have been simulated and verified with measurement.

## REFERENCES

1. Usha, P. and C. Krishnan, "Compact UWB planar antenna with triple band EMI reduction characteristics for WiMAX/WLAN/X-band satellite downlink frequency," *Progress In Electromagnetics Research M*, Vol. 61, 123–131, 2017.

2. Sarkar, D., K. V. Srivastava, and K. Saurav, "A compact microstrip-fed triple band-notched UWB monopole antenna," *IEEE Antennas and Wireless Propagation Letters*, Vol. 13, 396–399, 2014.

3. Wang, Z., G.-X. Zhang, Y. Yin, and J. Wu, "Design of a dual-band high-gain antenna array for WLAN and WiMAX base station," *IEEE Antennas and Wireless Propagation Letters*, Vol. 13, 1721–1724, 2014.

4. Lian, R., Z. Tang, and Y. Yin, "Design of a broadband polarization-reconfigurable Fabry-Perot resonator antenna," *IEEE Antennas and Wireless Propagation Letters*, Vol. 17, No. 1, 122–125, 2017.

5. Lalbakhsh, A. and K. P. Esselle, "Directivity improvement of a Fabry-Perot cavity antenna by enhancing near field characteristic," *2016 17th International Symposium on Antenna Technology and Applied Electromagnetics (ANTEM)*, IEEE, 2016.

6. Hayat, T., M. U. Afzal, F. Ahmed, et al., "Low-cost ultrawideband high-gain compact resonant cavity antenna," *IEEE Antennas and Wireless Propagation Letters*, Vol. 19, No. 7, 1271–1275, 2020.

7. Adibi, S., M. Amin Honarvar, and A. Lalbakhsh, "Gain enhancement of wideband circularly polarized UWB antenna using FSS," *Radio Science*, Vol. 56, No. 1, 1–8, 2021.

8. Zarbakhsh, S., M. Akbari, F. Samadi, and A.-R. Sebak, "Broadband and high-gain circularly-polarized antenna with low RCS," *IEEE Transactions on Antennas and Propagation*, Vol. 67, No. 1, 16–23, 2018.

9. Catton, G. D., H. G. Espinosa, A. A. Dewani, and S. G. O'keefe, "Miniature convoluted FSS for gain enhancement of a multiband antenna," *IEEE Access*, Vol. 9, 36898–36907, 2021.

10. Lalbakhsh, A., M. U. Afzal, K. P. Esselle, et al., "A high-gain wideband EBG resonator antenna for 60 GHz unlicenced frequency band," *12th European Conference on Antennas and Propagation (EuCAP 2018)*, IET, 2018.

11. Lalbakhsh, A., M. U. Afzal, T. Hayat, et al., "All-metal wideband metasurface for near-field transformation of medium-to-high gain electromagnetic sources," *Scientific Reports*, Vol. 11, No. 1, 9421, 2021.

12. Urul, B., "Gain enhancement of microstrip antenna with a novel DNG material," *Microwave and Optical Technology Letters*, Vol. 62, No. 4, 1824–1829, 2020.

13. Yuan, B., Y. H. Zheng, X. H. Zhang, B. You, and G. Q. Luo, "A bandwidth and gain enhancement for microstrip antenna based on metamaterial," *Microwave and Optical Technology Letters*, Vol. 59, No. 12, 3088–3093, 2017.

14. Kumar, S. and R. Kumari, "Bandwidth and gain-enhanced composite right/left-handed antenna for ultra-wideband applications," *International Journal of RF and Microwave Computer-Aided Engineering*, Vol. 30, No. 3, e22095, 2020.

15. Sumathi, K., S. Lavadiya, P. Yin, J. Parmar, and S. K. Patel, "High gain multiband and frequency reconfigurable metamaterial superstrate microstrip patch antenna for C/X/Ku-band wireless network applications," *Wireless Networks*, Vol. 27, 2131–2146, 2021.

16. Lalbakhsh, A., R. B. V. B. Simorangkir, N. Bayat-Makou, et al., "Advancements and artificial intelligence approaches in antennas for environmental sensing," *Artificial Intelligence and Data Science in Environmental Sensing*, 19–38, 2022.

17. Esfandiari, M., A. Lalbakhsh, P. N. Shehni, et al., "Recent and emerging applications of Graphene-based metamaterials in electromagnetics," *Materials and Design*, Vol. 221, 110920, 2022.

18. Dadgarpour, A., A. A. Kishk, and T. A. Denidni, "Gain enhancement of planar antenna enabled by array of split-ring resonators," *IEEE Transactions on Antennas and Propagation*, Vol. 64, No. 8, 3682–3687, 2016.

19. Zhou, Z. and Y. Li, "Effective epsilon-near-zero (ENZ) antenna based on transverse cutoff mode," *IEEE Transactions on Antennas and Propagation*, Vol. 67, No. 4, 2289–2297, 2019.

20. Shaw, T., D. Bhattacharjee, and D. Mitra, "Gain enhancement of slot antenna using zero-index metamaterial superstrate," *International Journal of RF and Microwave Computer-Aided Engineering*, Vol. 27, No. 4, e21078, 2017.

21. Xue, F., S. Liu, and X. Kong, "Single-layer high-gain planar lens antenna based on the focusing gradient metasurface," *2019 International Symposium on Antennas and Propagation (ISAP)*, 1–3, IEEE, 2019.

22. Usha, P. and C. Krishnan, "Epsilon near zero metasurface for ultrawide-band antenna gain enhancement and radar cross section reduction," *AEU-International Journal of Electronics and Communications*, Vol. 119, 153167, 2020.

23. Erfani, E., M. Niroo-Jazi, and S. Tatu, "A high-gain broadband gradient refractive index metasurface lens antenna," *IEEE Transactions on Antennas and Propagation*, Vol. 64, No. 5, 1968–1973, 2016.

24. Zhou, L., X. Chen, X. Duan, and J. Li, "FPA using a three-layer PSS for gain enhancement," *IET Microwaves, Antennas and Propagation*, Vol. 12, No. 3, 400–405, 2017.

25. Das, P., K. Mandal, and A. Lalbakhsh, "Beam-steering of microstrip antenna using single-layer FSS based phase-shifting surface," *International Journal of RF and Microwave Computer-Aided Engineering*, Vol. 32, No. 3, e23033, 2022.

26. Roy, S. and U. Chakraborty, "Gain enhancement of a dual-band WLAN microstrip antenna loaded with diagonal pattern metamaterials," *IET Communications*, Vol. 12, No. 12, 1448–1453, 2018.

27. Ghosh, A., V. Kumar, G. Sen, and S. Das, "Gain enhancement of triple-band patch antenna by using triple-band artificial magnetic conductor," *IET Microwaves, Antennas and Propagation*, Vol. 12, No. 8, 1400–1406, 2018.

28. Lalbakhsh, A., M. U. Afzal, K. P. Esselle, and S. L. Smith, "All-metal wideband frequency-selective surface bandpass filter for TE and TM polarizations," *IEEE Transactions on Antennas and Propagation*, Vol. 70, No. 4, 2790–2800, 2022.

29. Kumar, N., U. K. Kommuri, and P. Usha, "Mutual coupling reduction in multiband MIMO antenna using cross-slot fractal multiband EBG in the $E$-plane," *Progress In Electromagnetics Research C*, Vol. 132, 1–10, 2023.

30. Kumar, N. and K. Usha Kiran, "Meander-line electromagnetic bandgap structure for UWB MIMO antenna mutual coupling reduction in $E$-plane," *AEU-International Journal of Electronics and Communications*, Vol. 127, 153423, 2020.

31. Smith, D., D. Vier, T. Koschny, and C. Soukoulis, "Electromagnetic parameter retrieval from inhomogeneous metamaterials," *Physical Review E*, Vol. 71, No. 3, 036617, 2005.

32. Watts, C. M., X. Liu, and W. J. Padilla, "Metamaterial electromagnetic wave absorbers," *Advanced Materials*, Vol. 24, No. 23, OP98–OP120, 2012.